An octave spanning mid-infrared frequency comb generated in a silicon nanophotonic wire waveguide

Bart Kuyken[1,2], Takuro Ideguchi[3], Simon Holzner[3], Ming Yan[3,4], Theodor W. Hänsch[3,4], Joris Van Campenhout[5], Peter Verheyen[5], Stéphane Coen[6], Francois Leo[1,2], Roel Baets[1,2], Gunther Roelkens[1,2], Nathalie Picqué[3,4,7]

[1]Photonics Research Group, Department of Information Technology, Sint-Pietersnieuwstraat 41, Ghent University–imec, Ghent, Belgium
[2] Center for Nano- and Biophotonics (NB-Photonics), Ghent University, Ghent, Belgium
[3] Max Planck Institut für Quantenoptik, Hans-Kopfermann str. 1, 85748 Garching Germany
[4] Ludwig-Maximilians-Universität München, Fakultät für Physik, Schellingstr. 4/III, 80799 Munich, Germany
[5] imec, Kapeldreef 75, Leuven, Belgium
[6]Physics Department, The University of Auckland, Private Bag 92019, Auckland, New Zealand
[7] Institut des Sciences Moléculaires d'Orsay, CNRS, Bâtiment 350, 91405 Orsay, France

Abstract

Laser frequency combs, sources with a spectrum consisting of hundred thousands evenly-spaced narrow lines, have an exhilarating potential for new approaches to molecular spectroscopy and sensing in the mid-infrared region. The generation of such broadband coherent sources is presently under active exploration. Technical challenges have slowed down such developments. Identifying a versatile highly-nonlinear medium for significantly broadening a mid-infrared comb spectrum remains challenging. Here we take a new approach to spectral broadening of mid-infrared frequency combs and investigate CMOS-compatible highly nonlinear dispersion-engineered silicon nanophotonic waveguides on a silicon-on-insulator chip. We record octave-spanning (1,500-3,300 nm) spectra with a coupled input pulse energy as low as 16 pJ. We demonstrate the first phase-coherent comb spectra broadened on a CMOS-compatible chip. Our technique demonstrates new capabilities for room-temperature-operating integrated mid-infrared photonics and its applications and for supercontinuum generation on a chip.

Introduction

Frequency combs in the mid-infrared region [1] have been mostly generated by nonlinear frequency conversion of near-infrared frequency combs. Though the field is currently very active with the exploration of many different and promising approaches [2, 3, 4], producing a very broad spectrum with a slowly varying envelope remains challenging. Supercontinuum generation in a highly nonlinear fiber is known, under certain circumstances [5], to be a powerful way to generate an octave-spanning frequency comb. However, in the mid-infrared spectral region, suitable materials have remained scarse and difficult to engineer. Phase-coherent octave-spanning frequency comb generation has been achieved by spectral broadening of optical parametric oscillators [6] and thulium-doped fiber laser [7, 8, 9] frequency combs in nonlinear chalcogenide tapered fibers. The difficulty to produce such fragile chalcogenide fibers, the breakage of the fiber under high average pump power, as well as the deterioration of these glasses in the presence of moisture, render the approach challenging. However, taper lifetimes have recently been improved to several days with hybrid silica-chalcogenide structures, in which octave-spanning frequency comb generation has been reported [8, 9] using 65-fs pulses of only 18 pJ. Promising solutions for enhanced stability are presently under investigation with multimaterial chalcogenide nanotapers [10]. Another approach is the use of quasi-phase matched periodically-poled lithium niobate (PPLN) waveguides. Impressive results have been obtained and an octave spanning phase coherent supercontinuum has been generated [11]. However absorption between 2,500 nm and 2,800 nm and more importantly the limited transparency of lithium niobate beyond 4,500 nm, inhibits the scaling of the technology to longer wavelengths. Furthermore high energy pulses (7 nJ) are needed due to the moderate nonlinearity of the waveguide. Additionally, during the poling of the crystal small random variations on the location of the walls of the poled domains are

introduced. This aberration increases the conversion of parasitic processes significantly [11, 12] and makes modeling difficult.

Silicon-based waveguides have been originally conceived for the telecommunication region. In this region, octave-spanning supercontinuum generation has been demonstrated by pumping silicon nitride waveguides with 150-pJ pulses centered at 1.3 μm [13], but the coherence conservation in the supercontinuum generation process has not been investigated. Recently the application of silicon technology to the mid-infrared spectral region has attracted significant interest. Silicon nanophotonic wire waveguides can be engineered [14] within a nanometer precision in a standard CMOS facility. Such waveguides offer many advantages for mid-infrared nonlinear optics, mostly related to the wide transparency range of silicon (1.1-8 μm), its high nonlinear refractive index, the possibility of precise dispersion engineering of the waveguide platforms and the high refractive index contrast between the silicon waveguide core and the cladding material (typically SiO_2 or air), which allows for densely integrated waveguide systems with a nonlinear parameter an order to two orders of magnitude higher than possible in chalcogenide or silicon nitride systems. In this article, we report on the design of strongly nonlinear, dispersion controlled silicon photonic wire waveguides. We harness such chemically stable waveguides for mid-infrared supercontinuum generation and we demonstrate a phase-coherent frequency comb generator with a 30 dB bandwidth spanning from 1,540 nm up to 3,200 nm with coupled input pulse energies as low as 16 pJ.

Results

A highly nonlinear dispersion engineered silicon waveguide. The photonic wire is fabricated in a CMOS pilot line [14] on a 200-mm silicon-on-insulator (SOI) wafer and consisting of a 390-nm thick silicon device layer on top of a 2-μm buried oxide layer. The

inset in Figure 1a) shows a schematic cross section of the silicon photonic wire. The 1-cm-long air-clad photonic wire has a rectangular cross-section of 1,600 nm x 390 nm. The waveguide is slightly over etched by 10 nm into the buried oxide. The photonic wire widens near the cleaved facets to a 3-μm wide waveguide section for improved coupling efficiency. As a result of the high nonlinear index of silicon [15] and the strong optical confinement obtained by the high linear refractive index of silicon, the nonlinear parameter in the silicon wire is 38 $(Wm)^{-1}$ at 2,300 nm for the highly confined quasi-TE mode. Such high nonlinear parameter in silicon waveguides shows the advantage of using silicon over chalcogenide tapers (γ = 4.5 $(Wm)^{-1}$ [6]) and silicon nitride waveguides (γ = 1.2 $(Wm)^{-1}$ [13]) where the nonlinear parameter is much lower. As a result of the high confinement, the waveguide dispersion of the silicon photonic wire contributes strongly to the overall dispersion of the optical waveguide, such that group velocity dispersion can be engineered by optimizing the waveguide dimensions. The group velocity dispersion of the quasi-TE mode of the dispersion engineered photonic wire waveguide as a function of wavelength is shown in Figure 1a). The group velocity dispersion is simulated with the help of a finite element mode solver (Fimmwave). The zero dispersion wavelength is at 2,180 nm and the dispersion becomes positive (normal) at shorter wavelengths, while the dispersion remains low over a wide spectral band. By using a cut-back technique the propagation loss for the quasi-TE mode is determined to be < 0.2 $dB.cm^{-1}$ in the wavelength range of 2,200-2,400 nm.

The experimental setup for supercontinuum generation. The setup is shown in Figure 1 b). The frequency comb seed source consists of a homemade mid-infrared singly resonant optical parametric oscillator (OPO) [16] at a repetition frequency of 100 MHz, synchronously pumped by a femtosecond mode-locked Ti-Sapphire laser. The OPO is

tuned to a center wavelength of 2,290 nm, close to the zero dispersion wavelength of 2,180 nm of the silicon waveguide. Pumping a waveguide close to the zero dispersion wavelength in the anomalous region allows for broadband supercontinuum generation [5]. The OPO has a pulse duration of 70 fs (see Supplementary Fig. 1), while its average power is 35 mW. The ultra-short mid-infrared fs pulses coming from the OPO are coupled to the quasi-TE mode of the silicon photonic wire using a high NA (NA=0.85) chalcogenide lens with a focal length of 1.87 mm. The output of the chip is coupled, using another chalcogenide lens, to a Fourier transform spectrometer (FTS) to quantify the spectrum of the output pulses (see Supplementary Information). The coupling loss at the input waveguide facet is estimated to be 12 dB, leading to an on-chip peak power of 225 W or pulse-energy of 16 pJ. The high coupling loss at the waveguide facet stems from the bad overlap of the quasi-TE mode of the waveguide and the mode profile at the focus plane of the lens. However, spot size converters [17] could be used to significantly improve the coupling efficiency. We note that the coupled pulse energy and pulse duration that we use are similar to that used in [8] for phase-coherent supercontinuum generation in a chalcogenide-silica hybrid waveguide.

Spectral broadening in a silicon photonic nanowire waveguide. The spectra at the input and output of the waveguide are shown in Figure 2) for a pulse energy of 16 pJ. Spectra at lower pulse energies can be found in Supplementary Fig. 2. The spectrum of the pulses is significantly broadened in the silicon photonic wire waveguide and spans more than an octave: the 30 dB bandwidth spans from 1,540 nm up to 3,200 nm at the output. The peak at 1,600 nm is located in the normal dispersion regime of the waveguide and is generated through dispersive wave generation, a method used to spectrally extend a supercontinuum [18]. In the course of the several weeks of experimental investigations,

we did not observe any modification of the characteristics of the supercontinuum at the output of the silicon waveguide. Consistently, silicon-on-insulators platforms are used electronics [19] and optics [20] during years without degradation.

A phase coherent supercontinuum. We experimentally investigate the phase coherence of the supercontinuum generated in the waveguide by beat note measurements with a set of narrow line-width continuous-wave lasers. Such characterization technique for assessing comb coherence properties is entirely equivalent to that involving a *f*-2*f* interferometer [21] and it is well documented in the literature, e.g. [3, 4, 22]. Here, it was chosen because our foreseen applications [23] to molecular spectroscopy do not require self-referencing of the comb. In this characterization, all laser systems, including the continuous wave ones, are free-running. First, we beat the free-running seed source with a tunable continuous wave OPO (Argos Aculight, line-width ~60 kHz at 500 μs) at 2,400 nm on a fast InGaAsSb photodetector (Figure 3a)). We then beat the supercontinuum output with the same OPO (Figure 3b) and 3c) respectively), tuned at 2,418 and 2,580 nm. We finally beat (Figure 3 d)), on a fast InGaAs detector, the supercontinuum with a narrow line-width erbium doped fiber laser (Koheras AdjustiK E15, NKT Photonics, line-width 0.1 kHz at 100 μs) at 1,586 nm, far from the seed wavelength. All radio-frequency spectra are recorded with a 100-kHz resolution bandwidth, and a spectrum with a 105-MHz span shows three isolated lines. The strong beat signal at 100 MHz corresponds to the repetition frequency of the fs OPO, while the other two beat notes correspond to the beat signal generated by the continuous wave lasers and the two spectrally closest lines of the frequency comb. The line-width of the beat notes, measured with a 10-kHz resolution bandwidth (inset of the figures) is limited by the instabilities of the free-running lasers but it is found to be about 50 kHz, without noticeable broadening relative to the fs OPO seed

source. The width of the free-running beat notes is the convolution of the width of the two beating laser lines. However, the width of the lines of the free-running femtosecond mode-locked Ti-Sapphire laser used to synchronously pump the seed fs OPO is similar. Stabilizing the system against a radio-frequency reference, like a caesium clock, is not expected to bring significant line-width reduction: the locking electronics would need a bandwidth that only compensates for slow fluctuations (about 100 Hz) to avoid "coherence collapse" by multiplication of the phase noise of the radio-frequency reference [24]. We note that our measured line-widths are in full agreement with that of other free-running or radio-frequency-referenced frequency comb systems [24]. Additionally, we measured the relative line width of the comb lines located near the telecom wavelength by measuring the line width of the repetition rate of the pulses with the help of an high resolution spectrum anlyzer and an InGasAs photo detector. As can be seen in Figure 4, the RF spectrum in the vicinity of the repetition rate is clean. Furthermore, the measure line width of the RF tone, shown in the inset, is limited by the 1 Hz resolution of the RF spectrum analyzer. Our investigation thus demonstrates the frequency comb structure of the supercontinuum.

Comparison with simulations. The coherence of the supercontinuum can be simulated and such simulations can be used to confirm the frequency comb structure at the probed wavelengths as well as indicating the coherence over the whole bandwidth. The supercontinuum generation can be simulated by solving the generalized nonlinear Schrödinger equation numerically with a split step Fourier method [5] (see methods). The simulation takes the linear propagation loss, the nonlinear phase shift, the three photon absorption and both the induced absorption and dispersion by the carriers into account. In the simulation the nonlinear parameter γ is assumed to be 38 $(Wm)^{-1}$, the linear

propagation loss is assumed to be 0.1 dB.cm^{-1} and the three photon absorption coefficient is assumed to be 0.025 cm^{3}.GW^{-2} [25]. Figure 5 a) shows the evolution of the spectrum of a 225-W peak power, 70-fs long pulse as it is propagating along the silicon photonic wire waveguide. The simulated spectrum after 1-cm propagation is shown in Figure 5b). As shown in the figure, the simulation agrees very well with the experimental results. The simulation of the spectral evolution of the pulse along the photonic wire length reveals (Fig. 5 a)) that in the first millimeter of propagation the spectrum is primarily broadened due to self phase modulation. The spectrum is further broadened into the telecom wavelength range, where the group velocity dispersion of the waveguide is normal, through dispersive wave generation [26]. The use of the short pulses favors the processes such as dispersive wave generation and self-phase modulation. Unlike in [27] where longer, ps pulses were used and the spectral broadening primarily results of amplification of background noise (modulation instability) the nonlinear process of dispersive wave generation and self-phase modulation maintain the coherence in the pulse. These nonlinear processes are not specific to the pump wavelength. For example our simulations (see also Supplementary Fig. 3) show that a thulium doped mode-locked fiber laser can be used as well to generate an (phase coherent) octave spanning supercontinuum in a dispersion engineered silicon waveguide.

The coherence of the supercontinuum can be simulated, by including shot noise at the input. The noise $E_{noise}(t)$ at the input is assumed to be a random variable with a stochastic distribution $< E_{noise}(t)\, E_{noise}(t+\tau)> = \frac{h\upsilon}{2}\delta(t)$, with h the Planck constant and υ the frequency of the photons, and analyzing an ensemble of simulated supercontina [28]. The first order coherence function

$$g_{12}(\omega) = \frac{\left| < E_i(\omega) E_j(\omega) >_{i \neq j} \right|}{\sqrt{< \left|E_i(\omega)\right|^2 >< \left|E_j(\omega)\right|^2 >}}$$

is calculated for an ensemble of 100 spectra and is shown in Figure 5c). The coherence is close to unity over the whole spectrum, indicating that the generated supercontinuum is coherent over its entire bandwidth.

To emphasize the comb structure of the supercontinuum spectrum, which results from the pulse-to-pulse coherence, the spectrum of the pulse train at the output of the chip was simulated with a resolution of 10 kHz in a narrow band interval. The spectrum is simulated by first generating a set of pulses including the input shot noise, but excluding timing jitter and residual intensity noise, as discussed above. These pulses were stacked together in a pulse train with a repetition frequency of 100 MHz. The Fourier transform was calculated to generate the spectrum of the pulse train (see Supplementary Information for details). Figure 6 shows the spectrum of a train of 1,000 pulses, calculated in a 500-MHz interval at 1,586 nm. The independent comb lines can clearly be seen. The inset of Figure 6 shows one individual comb line sampled with a resolution of 10 kHz by calculating the spectrum of a pulse train consisting of 10,000 pulses. Similar simulations were done in an interval at 2,418 nm and 2,580 nm confirming the comb structure of the supercontinuum (see Supplementary Fig. 5). In the simulations, the width of the comb lines is only limited by the time window used.

Discussion

Using a silicon nanowire on a chip, we have demonstrated an octave-spanning frequency comb spanning from the telecom wavelength window around 1,500 nm to the mid-infared wavelength range at 3,300 nm. Such frequency comb is readily suitable for direct frequency comb spectroscopy, particularly for dual-comb spectroscopy with e.g. adaptive sampling [23]. Improved dispersion engineering could potentially extend the supercontinuum over the whole transparency window of the SOI platform (1,100 nm to

4,000 nm), limited by the buried oxide. Even broader bandwidths could be further obtained up to 5,500 nm with silicon on sapphire waveguide platforms [29, 30]. By using waveguide designs where the buried oxide is removed [31, 32, 33] the entire silicon transparency window (up to 8,500 nm) could be covered. As many molecules have strong rovibrational lines in the mid-infrared range, such developments would contribute in expanding the intriguing capabilities of molecular spectroscopy with frequency combs to the molecular fingerprint region. Such broadband supercontinua may also lead to self-referenced mid-infrared frequency comb systems, as needed for precision measurements in frequency metrology and in some implementations of direct frequency comb spectroscopy [1]. The rapid progress in the development of miniaturized mid-infrared frequency comb generators, as reported for instance with quantum cascade lasers [2, 4] or high-quality factor micro-resonators [34], might lead to an entirely new strategy for a compact source of ultrashort pulses in the future. Our work would then represent an essential building block paving the road for an octave-spanning frequency comb entirely generated on a chip. Such prospect would be of interest to e.g. chemical sensing, calibration of astronomical spectrographs, environmental monitoring or free-space communications.

Methods:

Description of the mid-infrared frequency comb seed source. The frequency comb generator that seeds the silicon waveguide is a home-made femtosecond synchronously-pumped optical parametric oscillator

(OPO). Its design and characterization are described in [16]. Here we just reproduce the details that are useful for the description of the present experiment. The pump source of the OPO is a Kerr-lens mode-locked Ti:sapphire oscillator with a repetition frequency of 100 MHz, an average power of 1 W, a central wavelength of 790 nm and a pulse duration of 20 fs. The nonlinear crystal of the OPO is made of MgO:PPLN with an fan-out grating interaction length of l=500 μm. The OPO cavity is a dispersion-controlled four-mirror standing-wave design with two plano-concave mirrors and four plane mirrors. We tune the central wavelength of the idler of the OPO to 2,290 nm. The average output power is 35 mW. The idler spectrum is shown in Fig. 2b. We measure the pulse duration with a home-made autocorrelator based on two-photon absorption in a InGaAs photodetector. The autocorrelation (Supplementary Fig. 1) reveals a pulse duration of 72 fs, assuming a $sech^2$ profile.

Simulations. The spectral evolution of the pulses along the waveguide is simulated by solving the generalized nonlinear Schrodinger equation numerically using a split-step approach [35]. We solve

$$\frac{\partial E(z,t)}{\partial z} = i\sum_{k\geq 2} i^k \frac{\beta_k}{k!}\frac{\partial^k E}{\partial t^k} - \frac{\alpha_l}{2}E - \frac{\alpha_{3eff}}{2}|E|^4 E - \alpha_c(1+\mu i)E + i\gamma(1+\frac{i}{\omega_0}\frac{\partial}{\partial t})E\int_{-\infty}^{t} R(t-t')\left|E(z,t')\right|^2 dt'$$

Here E(z,t) is the envelope of the electric field of the short pulses, β_k is the kth order dispersion coefficient, α_l the linear propagation loss, α_{3eff} the effective third order absorption coefficient, α_c the free carrier absorption coefficient, μ takes the free carrier dispersion in account, γ is the nonlinear parameter of the waveguide, while the integral takes in account the fractional Raman response. The effective third order absorption coefficient can be calculated as $\alpha_{3eff} = \frac{n_g^2 \alpha_3}{n^2 A_{5eff}^2}$ [36] where α_3 is the third order nonlinear absorption coefficient in silicon of about $2.5\text{x}10^{-26}\text{m}^3.\text{GW}^{-2}$ [37, 25] and A_{5eff}=0.5 μm^2 the fifth order mode area . The carrier induced absorption coefficient is proportional to the carrier density N_c, such that $\alpha_c = \sigma N_c$, where $\sigma = 2.77\text{x}10^{-21}$ m^2 [38], while $\mu = \frac{2k_c}{\sigma\omega_0 c}$ with $k_c = 1.35\text{x}10^{-27}$ m^3 [38]. The evolution of the carrier density itself can be calculated as $\frac{\partial Nc(z,t)}{\partial t} = \frac{2\pi\alpha_{3eff}}{3h\omega}\frac{|E(z,t)|^6}{A_{eff}} - \frac{N_c(z,t)}{\tau}$ [38] where h is Planck's constant and τ the carrier lifetime, estimated to be 1 ns [39]. It was assumed that the pulse was a hyperbolic secant with a FWHM of 70 fs.

References

[1] Schliesser, A., Picqué, N. & Hänsch, T.W. Mid-infrared frequency combs. *Nature Photon.* **6**, 440-449 (2012).

[2] Hugi, A., Villares, G., Blaser, S., Liu, H., & Faist, J. Mid-infrared frequency comb based on a quantum cascade laser. *Nature* **492,** 229-233 (2012).

[3] Wang, C. *et al.* Mid-infrared optical frequency combs at 2.5 μm based on crystalline microresonators. *Nature Comm.* **4**, 1-7 (2013).

[4] Burghoff, D. *et al*. Terahertz laser frequency combs. *Nature Phot.* **8**, 462-467 (2014).

[5] Dudley, J. M., Genty, G. & Coen, S. Supercontinuum generation in photonic crystal fiber. *Rev. Mod. Phys.* **78**, 1135-1184 (2006).

[6] Rudy, C. W., Marandi, A., Vodopyanov, K. L. & Byer, R. L. Octave-spanning supercontinuum generation in in situ tapered As_2S_3 fiber pumped by a thulium-doped fiber laser. *Opt Lett.* **38,** 2865-2868 (2013).

[7] Lee, K. *et al.* Mid-infrared frequency combs from coherent supercontinuum in chalcogenide nanospike. *Opt. Lett.* **39**, 2056-2059 (2014).

[8] Granzow, N. *et al.* Mid-infrared supercontinuum generation in As2S3-silica "nano-spike" step-index waveguide. *Opt. Express* **21**, 10969-10977 (2013).

[9] Shabahang, S. et al . *CLEO: 2013, OSA Technical Digest.* paper SW3I.2 *(Optical Society of America, 2013)*

[10] Phillips, C. R. *et al.* Supercontinuum generation in quasi-phase-matched $LiNbO_3$ waveguide pumped by a Tm-doped fiber laser system. *Opt Lett.* **36,** 3912-3914 (2011).

[11] Phillips, C. R, Pelc, J. S., & Fejer, M. M. Parametric processes in quasi-phasematching gratings with random duty cycle errors. *J. Opt. Soc. Am. B* **30,** 982-993 (2013).

[12] Halir., R. *et al.* Ultrabroadband supercontinuum generation in a CMOS-compatible platform. *Opt. Lett.* **37**, 1685-1687 (2012).

[13] Bogaerts, W. *et al.* Nanophotonic waveguides in silicon-on-insulator fabricated with CMOS technology. *J. Lightw. Technol.* **23**, 401-412 (2005).

[14] Bristow, A. D., Rotenberg N., & Van Driel, H. M. Two-photon absorption and Kerr coefficients of silicon for 850-2200 nm. *Appl. Phys. Lett.* **90**, 191104 (2007).

[15] Marandi A. *et al.* Mid-infrared supercontinuum generation in tapered chalcogenide fiber for producing octave-spanning frequency comb around 3 μm. *Opt. Express* **20**, 24218-24225 (2012).

[16] Kumar, S. C. *et al.* Few-cycle, broadband, mid-infrared optical parametric oscillator pumped by a 20-fs Ti:sapphire laser. *Laser Photon. Rev.* ***8***, L86-L91 (2014).

[17] Pu, M., Liu L., Ou, H., Yvind K., Hvam, J. M. Ultra-low-loss inverted taper coupler for silicon-on-insulator ridge waveguide. *Opt. Comm.* **283**, 3678-3682 (2010).

[18] Lau, R. *et al.* Octave-spanning mid-infrared supercontinuum generation in silicon nanowaveguides. *Opt. Lett.* **39**, 4518-4525 (2014).

[19] Colinge J. *Silicon-on-Insulator Technology: Materials to VLSI*. (Kluwer Academic Publishers , 2004).

[20] Hochberg, M., Jones, T. B. Towards Fabless silicon photonics. *Nature Photon.* **4**, 492-494 (2010).

[21] Udem, T., Holzwarth, R. & Hänsch, T. Optical Frequency Metrology. *Nature* **416**, 233-237 (2002).

[22] Gohle C. *et al.* A frequency comb in the extreme ultraviolet. *Nature* **436**, 234-237 (2005).

[23] Ideguchi, T. *et al.* Adaptive real-time dual-comb spectroscopy. *Nature Comm.* **5**, 3375 (2014).

[24] Diddams, S. A., Ye, J., & Hollberg L. *Femtosecond lasers for optical clocks and low noise frequency synthesis* in *Femtosecond optical frequency comb: principle, operation and applications*, (eds J. Ye & S. T. Cundiff), 225–262 (Springer, 2005).

[25] Pearl, S., Rotenberg, N. & Driel, H. M. Three photon absorption in silicon for 2300-3300 nm. *Appl. Phys. Lett.* 93, 131102 (2008).

[26] Cristiani, I., Tediosi, R., Tartara, L., & Degiorgio, V. Dispersive wave generation by solitons in microstructured optical fibers. *Opt. Express* **12,** 124-135 (2004).

[27] Kuyken, B. *et al*. Mid-infrared to telecom-band supercontinuum generation in highly nonlinear silicon-on-insulator wire waveguides. *Opt. Express* **19,** 20172-20181(2011).

[28] Ruehl, A. *et al*. Ultrabroadband coherent supercontinuum frequency comb. *Phys. Rev. A* **84**, 11806-11811 (2011).

[29] Baehr-Jones, T. *et al.* Silicon-on-sapphire integrated waveguides for the mid-infrared. *Opt Express* **18**, 12127-12135 (2010).

[30] Li, F. *et al.* Low propagation loss silicon-on-sapphire waveguides for the mid-infrared. *Opt. Express* **19,** 15212-15220 (2011).

[31] Soref, R., Emelett A. & Buchwald, W. R. Silicon waveguided components for the long-wave infrared region. *J Opt A-Pure Appl Op* **8**, 840-853 (2006).

[32] Soref, R. Mid-infrared photonics in silicon and germanium. *Nature Photon*. **4**, 495-497 (2010).

[33] Jalali, B. Nonlinear optics in the mid-infrared. *Nature Photon*. **4**, 506-508 (2010).

[34] Griffith, A. G. *et al.* Silicon-chip mid-infrared frequency comb generation. *arXiv* 1408.1039 (2014).

[35] Yin, L., Lin, Q., & Agrawal, G. P. Soliton fission and supercontinuum generation in silicon waveguides. *Opt. Lett.* **32,** 391-393 (2007).

[36] Husko, C. , et al. Non-trivial scaling of self-phase modulation and three-photon absorption in III–V photonic crystal waveguides. *Opt. Express* **17**, 22442-22451 (2009).

[37] Gai, X. *et al.* Nonlinear absorption and refraction in crystalline silicon in the mid-infrared. *Laser Photon. Rev*. **7**, 1054-1064 (2013).

[38] Lin, Q., Painter, O. J., & Agrawal, G. P. Nonlinear optical phenomena in silicon waveguides: modeling and applications. *Opt. Express*, vol. 15, no. 25, pp. 16604-16644 (2007).

[39] Boyraz, O., Koonath, P., Raghunathan, V. & Jalali B. All optical switching and continuum generation in silicon waveguides. *Opt. Express* **12**, 4094-4102 (2004).

Acknowledgements

B. Kuyken acknowledges the special research fund of Ghent University (BOF), for a post doctoral fellowship. We are grateful to Dr. Antonin Poisson and Dr. Clément Lafargue for experimental support. This work was partly carried out in the framework of the Methusalem project “Smart Photonic Chips” and the FP7-ERC-INSPECTRA, FP7-ERC-MIRACLE and FP7-ERC-Multicomb (Advanced Investigator Grant 267854) projects.

Contributions

B.K. performed the numerical dispersion design calculations with guidance from R.B. and G.R., J.V.C and P.V. supervised the waveguide device fabrication process. B.K, T.I, S.H.

and M.Y performed the supercontinuum generation experiment as well as the beatnote experiment with guidance and supervision from T.H. and N.P. T.I, S.H. and M.Y performed the autocorrelation experiment under the supervision of N.P. B.K., F.L. and S.C. performed the simulations on the coherence. B.K. drafted the manuscript. All authors provided comments and suggestions for improvements.

Competing financial interests

The authors declare no competing financial interests.

Author information

Correspondence and requests for materials should be addressed to B.K. (Bart.Kuyken@intec.ugent.be).

Figure legends

Figure 1: a) The simulated dispersion of the quasi TE-mode of the photonic wire waveguide and b) the experimental setup. a) The zero-dispersion wavelength is at 2,180 nm, while the dispersion is normal at shorter wavelengths and anomalous at longer wavelengths. The waveguide cross-section is shown in the inset. b) experimental setup: the OPO pumped by a Ti-Sapphire mode-locked laser is coupled to the silicon chip with a lens. The output of the chip can be sent to a photodetector or a spectrometer.

Figure 2: The spectrum at the input (red) and the output (black) of the silicon nanowire. The input pulses are centered at 2,290 nm and have a coupled peak power of 225 W. Their spectrum is broadened in the silicon photonic wire such that it spans more than an octave: the 30 dB bandwidth spans from 1,540 nm to 3,200 nm. The arrows indicate the wavelength position where the phase coherence measurements are performed.

Figure 3: RF spectra showing the narrow line-width beat notes of the input pulses (a) and output pulses (b,c,d). a) RF spectrum of the free-running beat note of the pump pulses and a narrow line-width source at 2,400 nm. b),c),d): free-running beat notes of the spectrally broadened pulses and a narrow line-width source at λ=2,418 nm, λ=2,580 nm and λ=1,586 nm, respectively. The insets in the figure show a high resolution spectrum of the free-running beat notes. The free-running beat notes of the output pulses are measured

to be about 50 kHz wide and are not broadened as compared to beat notes measured on the input pulses.

Figure 4: The RF spectrum in the vicinity of the repetition rate frequency. The inset shows the line width measured with a high resolution RF spectrum analyzer. The line width is limited by its 1 Hz resolution.

Figure 5: The simulated spectral broadening in the silicon photonic wire waveguide and the coherence of the pulses. a) Evolution of the spectral content of the optical pulse along the length of the waveguide. b) Simulated spectra after 1 cm of propagation in the silicon photonic wire waveguide (blue) and the measured supercontinuum (red). c) Simulated coherence as a function of wavelength.

Figure 6: A high resolution spectrum of the broadened output pulses simulated in the vicinity of 1,586 nm (198 THz). The spectrum, simulated over a 500-MHz bandwidth, reveals the comb lines separated by 100 MHz in the supercontinuum frequency comb. A high resolution (10 kHz) inset around a comb line is also shown.

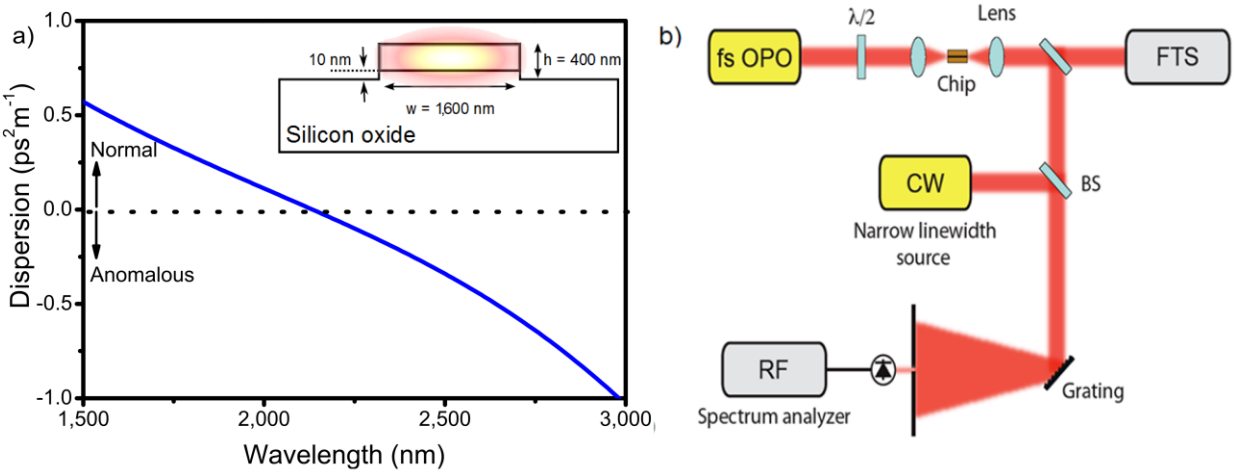
a)
1.0
0.5
0.0
-0.5
-1.0
Dispersion (ps^{2}m^{-1})
Normal
Anomalous
10 nm
h = 400 nm
w = 1,600 nm
Silicon oxide
1,500
2,000
2,500
3,000
Wavelength (nm)
b)
fs OPO
λ/2
Lens
Chip
FTS
CW
BS
Narrow linewidth source
RF
Spectrum analyzer
Grating

Figure 1

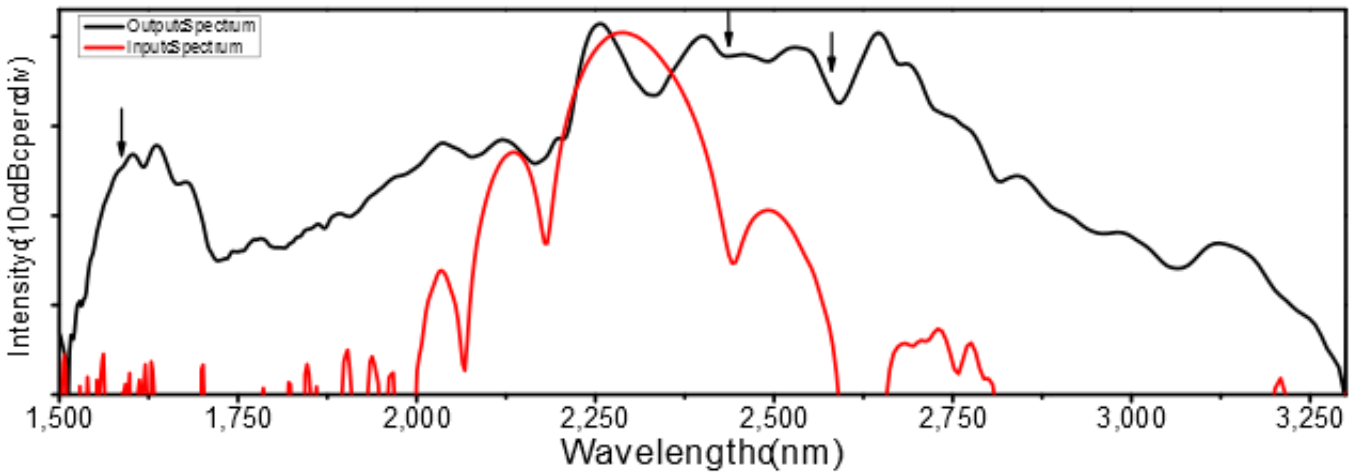
Output Spectrum
Input Spectrum
Intensity (10 dBc per div)
1,500
1,750
2,000
2,250
2,500
2,750
3,000
3,250
Wavelength (nm)

Figure 2

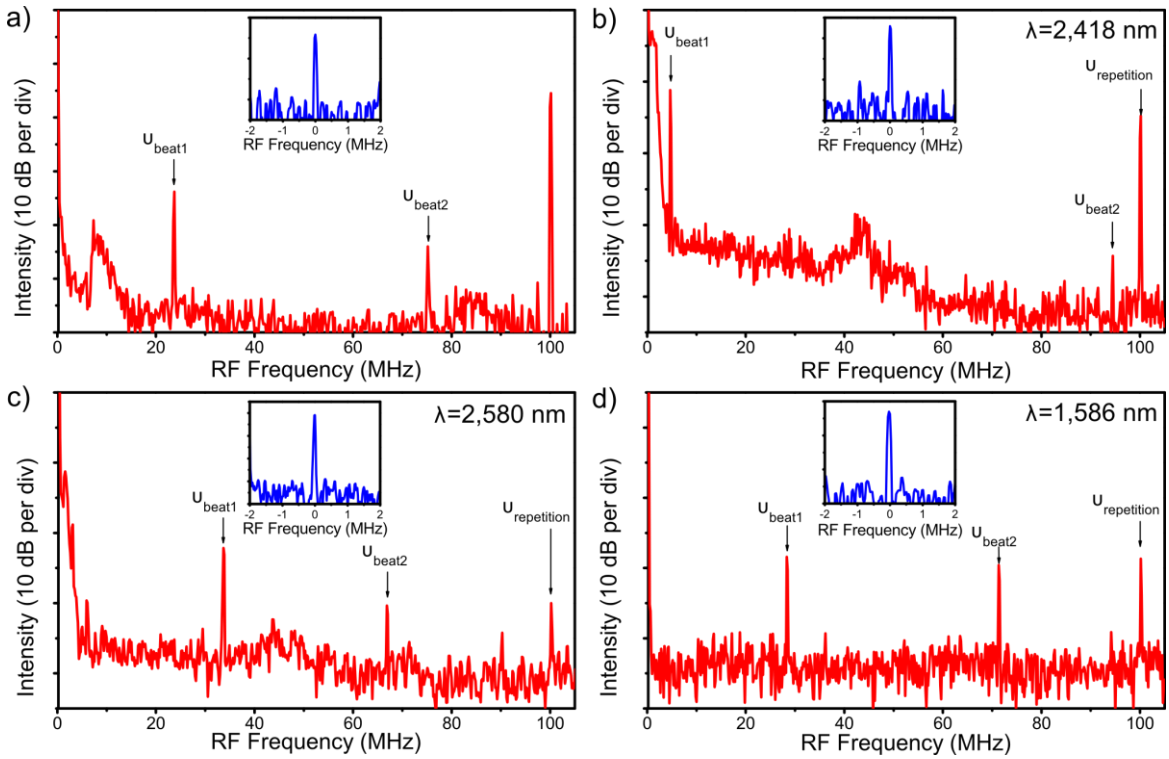
a)
b)
c)
d)
λ=2,418 nm
λ=2,580 nm
λ=1,586 nm
U beat1
U beat2
U repetition
RF Frequency (MHz)
Intensity (10 dB per div)

Figure 3

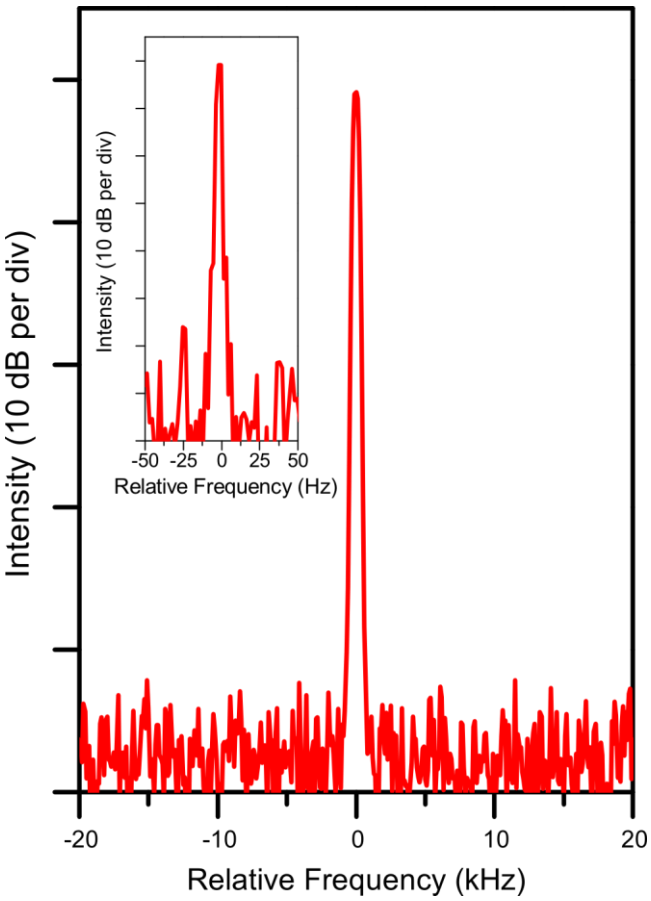
Intensity (10 dB per div)
-20
-10
0
10
20
Relative Frequency (kHz)
Intensity (10 dB per div)
-50 -25 0 25 50
Relative Frequency (Hz)
Figure 4

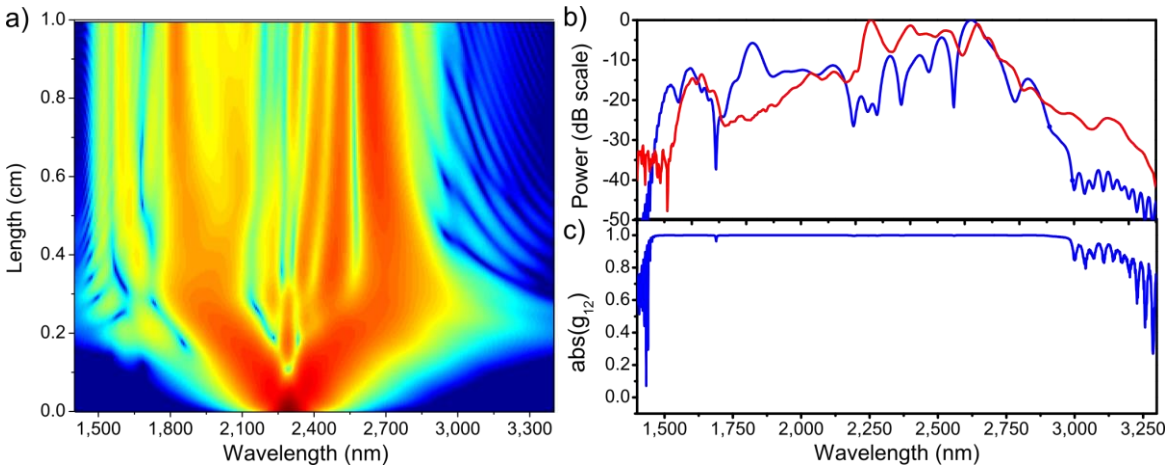
a)
Length (cm)
1.0
0.8
0.6
0.4
0.2
0.0
1,500
1,800
2,100
2,400
2,700
3,000
3,300
Wavelength (nm)
b)
Power (dB scale)
0
-10
-20
-30
-40
-50
c)
abs(g12)
1.0
0.8
0.6
0.4
0.2
0.0
1,500
1,750
2,000
2,250
2,500
2,750
3,000
3,250
Wavelength (nm)

Figure 5

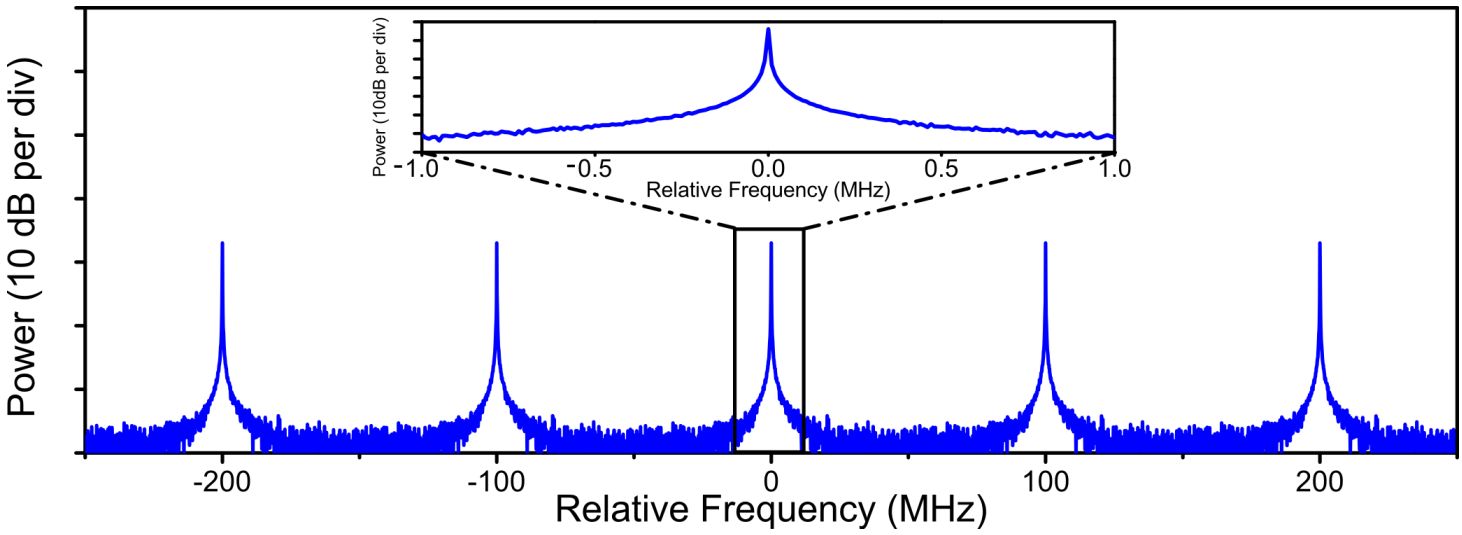
Power (10 dB per div)
-200
-100
0
100
200
Relative Frequency (MHz)
Power (10dB per div)
-1.0
-0.5
0.0
0.5
1.0
Relative Frequency (MHz)

Figure 6